

See discussions, stats, and author profiles for this publication at: <https://www.researchgate.net/publication/231732643>

# Gold(I) Hydride Intermediate in Catalysis: Dehydrogenative Alcohol Silylation Catalyzed by Gold(I) Complex

ARTICLE *in* ORGANOMETALLICS · AUGUST 2009

Impact Factor: 4.13 · DOI: 10.1021/om900445w

---

CITATIONS

56

---

READS

35

5 AUTHORS, INCLUDING:



[Hajime Ito](#)

Hokkaido University

128 PUBLICATIONS 2,393 CITATIONS

[SEE PROFILE](#)



[Chongmin Zhong](#)

Northwest A & F University

23 PUBLICATIONS 502 CITATIONS

[SEE PROFILE](#)

## Gold(I) Hydride Intermediate in Catalysis: Dehydrogenative Alcohol Silylation Catalyzed by Gold(I) Complex

Hajime Ito,<sup>\*,†,‡</sup> Tomohisa Saito,<sup>†</sup> Takahiro Miyahara,<sup>†</sup> Chongmin Zhong,<sup>†</sup> and Masaya Sawamura<sup>†</sup><sup>†</sup>Department of Chemistry, Faculty of Science, Hokkaido University, Sapporo 060-0810, Japan, and  
<sup>‡</sup>PRESTO, Japan Science and Technology Agency (JST), Honcho, Kawaguchi, Saitama 332-0012, Japan

Received May 26, 2009

Gold hydride is a rare transition-metal species. Despite the fact that gold hydrides may be key intermediates in several gold-catalyzed reactions, their chemical properties are not well understood. We report the synthesis, characterization, and catalytic properties of the gold(I) hydride species that play an important role in a gold(I)-catalyzed dehydrogenative alcohol silylation. Tricoordinated complexes AuCl(xantphos) (**1a**) and AuCl(xy-xantphos) (**1b**) were prepared and characterized by <sup>1</sup>H and <sup>31</sup>P{<sup>1</sup>H} NMR measurements and X-ray crystallography. Gold(I) hydride species **6b** generated from the reaction between **1b** and PhMe<sub>2</sub>SiH (**4b**) in CDCl<sub>3</sub> was characterized by <sup>1</sup>H and <sup>31</sup>P NMR measurements and ESI-MS spectrometry. NMR and kinetic studies revealed that the reaction mechanism involves the gold(I) hydride species as a key intermediate. The high catalytic activities of **1a** and **1b** in dehydrogenative alcohol silylation are explained by the stability of the tricoordinated chelating structure and the activation of the Au–Cl bond induced by the stereoelectronic effect of the coordinating phosphorus atoms. This study reports the first example of a gold(I) hydride complex that exhibits catalytic activity.

## Introduction

Transition-metal hydrides are very important intermediates in transition-metal-catalyzed hydrogenation, hydrosilylation, and other metal hydride-mediated catalysis. Extensive studies

have been conducted on the hydride derivatives of almost all transition-metal elements in an effort to understand their properties in catalytic reactions. Gold, a noble transition metal, which was once not considered to have a rich chemistry for organic transformations, is now attracting considerable attention in the area of homogeneous and heterogeneous catalysis.<sup>1–3</sup> Similar to other transition metals, intermediates containing Au–H structure are thought to be key intermediates in gold-catalyzed reactions:<sup>1a,1f,1g</sup> hydrogenation,<sup>3b,3c,5</sup> hydrosilylation,<sup>4a</sup> dehydrogenative silylation of alcohols,<sup>6</sup> hydroboration,<sup>7</sup> C–H bond activation,<sup>8</sup> aerobic oxidation of alcohols,<sup>9</sup> and dehydrogenative dimerization of

\*Corresponding author. E-mail: hajito@sci.hokudai.ac.jp.

(1) For recent reviews of gold catalysis, see: (a) Hashmi, A. S. K. *Angew. Chem., Int. Ed.* **2005**, *44*, 6990–6993. (b) Hashmi, A. S. K.; Hutchings, G. J. *Angew. Chem., Int. Ed.* **2006**, *45*, 7896–7936. (c) Gorin, D. J.; Toste, F. D. *Nature* **2007**, *446*, 395–403. (d) Hashmi, A. S. K. *Chem. Rev.* **2007**, *107*, 3180–3211. (e) Arcadi, A. *Chem. Rev.* **2008**, *108*, 3266–3325. (f) Gorin, D. J.; Sherry, B. D.; Toste, F. D. *Chem. Rev.* **2008**, *108*, 3351–3378. (g) Hashmi, A. S. K.; Rudolph, M. *Chem. Soc. Rev.* **2008**, *37*, 1766–1775. (h) Jiménez-Núñez, E.; Echavarren, A. M. *Chem. Rev.* **2008**, *108*, 3326–3350. (i) Li, Z.; Brouwer, C.; He, C. *Chem. Rev.* **2008**, *108*, 3239–3265. (j) Marion, N.; Nolan, S. P. *Chem. Soc. Rev.* **2008**, *37*, 1776–1782. (k) Patil, N. T.; Yamamoto, Y. *Chem. Rev.* **2008**, *108*, 3395–3442.

(2) For examples of pioneering works on gold catalysis, see: (a) Hutchings, G. J. *J. Catal.* **1985**, *96*, 292–295. (b) Ito, Y.; Sawamura, M.; Hayashi, T. *J. Am. Chem. Soc.* **1986**, *108*, 6405–6406. (c) Haruta, M.; Kobayashi, T.; Sano, H.; Yamada, N. *Chem. Lett.* **1987**, *16*, 405–408. (d) Fukuda, Y.; Utimoto, K. *Bull. Chem. Soc. Jpn.* **1991**, *64*, 2013–2015. (e) Teles, J. H.; Brode, S.; Chabanas, M. *Angew. Chem., Int. Ed.* **1998**, *37*, 1415–1418. (f) Hashmi, A. S. K.; Schwarz, L.; Choi, J. H.; Frost, T. M. *Angew. Chem., Int. Ed.* **2000**, *39*, 2285–2288. (g) Kennedy-Smith, J. J.; Staben, S. T.; Toste, F. D. *J. Am. Chem. Soc.* **2004**, *126*, 4526–4527. (h) Nieto-Oberhuber, C.; Muñoz, M. P.; Buñuel, E.; Nevado, C.; Cárdenas, D. J.; Echavarren, A. M. *Angew. Chem., Int. Ed.* **2004**, *43*, 2402–2406. (i) Zhang, J. L.; Yang, C. G.; He, C. *J. Am. Chem. Soc.* **2006**, *128*, 1798–1799.

(3) For selected examples of gold-catalyzed hydrogenations, see: (a) Claus, P. *Appl. Catal., A* **2005**, *291*, 222–229. (b) González-Arellano, C.; Corma, A.; Iglesias, M.; Sánchez, F. *Chem. Commun.* **2005**, 3451–3453. (c) Comas-Vives, A.; González-Arellano, C.; Corma, A.; Iglesias, M.; Sánchez, F.; Ujaque, G. *J. Am. Chem. Soc.* **2006**, *128*, 4756–4765. (d) Corma, A.; Serna, P. *Science* **2006**, *313*, 332–334. (e) Corma, A.; Concepción, P.; Serna, P. *Angew. Chem., Int. Ed.* **2007**, *46*, 7266–7269. (f) Corma, A.; Serna, P.; Garcka, H. *J. Am. Chem. Soc.* **2007**, *129*, 6358–6359. (g) Grirrane, A.; Corma, A.; Garcka, H. *Science* **2008**, *322*, 1661–1664. For other publications for gold-catalyzed hydrogenation including earlier works, see ref 1b.

(4) For gold-catalyzed hydrosilylations, see: (a) Ito, H.; Yajima, T.; Tateiwa, J.; Hosomi, A. *Chem. Commun.* **2000**, 981–982. (b) Caporusso, A.; Aronica, L.; Schiavi, E.; Martra, G.; Vitulli, G.; Salvadori, P. *J. Organomet. Chem.* **2005**, *690*, 1063–1066. (c) Corma, A.; González-Arellano, C.; Iglesias, M.; Sánchez, F. *Angew. Chem., Int. Ed.* **2007**, *46*, 7820–7822. (d) Debono, N.; Iglesias, M.; Sánchez, F. *Adv. Synth. Catal.* **2007**, *349*, 2470–2476. (e) Lantos, D.; Contel, M.; Sanz, S.; Bodor, A.; Horváth, I. T. *J. Organomet. Chem.* **2007**, *692*, 1799–1805. (f) Wile, B. M.; McDonald, R.; Ferguson, M. J.; Stradiotto, M. *Organometallics* **2007**, *26*, 1069–1076.

(5) For examples of hydrogenation reactions in which the intermediates with Au–H structures were proposed, see: (a) Boronat, M.; Concepción, P.; Corma, A.; González, S.; Illas, F.; Serna, P. *J. Am. Chem. Soc.* **2007**, *129*, 16230–16237. (b) Bus, E.; Prins, R.; van Bokhoven, J. A. *Catal. Commun.* **2007**, *8*, 1397–1402. (c) Corma, A.; Boronat, M.; González, S.; Illas, F. *Chem. Commun.* **2007**, 3371–3373. (d) Segura, Y.; López, N.; Pérez-Ramírez, J. *J. Catal.* **2007**, *247*, 383–386. (e) Comas-Vives, A.; González-Arellano, C.; Boronat, M.; Corma, A.; Iglesias, M.; Sánchez, F.; Ujaque, G. *J. Catal.* **2008**, *254*, 226–237. (f) Su, F. Z.; He, L.; Ni, J.; Cao, Y.; He, H. Y.; Fan, K. N. *Chem. Commun.* **2008**, 3531–3533. (g) Amir-Ebrahimi, V.; Rooney, J. J. *Catal. Lett.* **2009**, *127*, 20–24.

(6) For gold(I)-catalyzed dehydrogenative silylation of alcohols, see: (a) Ito, H.; Takagi, K.; Miyahara, T.; Sawamura, M. *Org. Lett.* **2005**, *7*, 3001–3004. (b) Raffa, P.; Evangelisti, C.; Vitulli, G.; Salvadori, P. *Tetrahedron Lett.* **2008**, *49*, 3221–3224.

trialkylstananes.<sup>10</sup> However, to the best of our knowledge, there have been no detailed characterizations of gold hydride complexes that show catalytic activity and little information on the chemical behavior of gold hydride species in catalysis.

One major obstacle in the progress of gold chemistry is the difficulty in preparing gold hydride species. Gold hydrides themselves have attracted considerable attention over the last few decades, primarily due to their unique structural properties.<sup>11</sup> Many experimental and theoretical investigations have been described on the structure of gold(I) or gold(III) hydride compounds.<sup>12</sup> The simplest gold(I) hydride molecule (AuH) and the related polyhydride molecules (AuH<sub>n</sub>, etc.) were generated in the gas phase and have been subjected to matrix isolation for characterization.<sup>13,14</sup> These species are unstable under typical catalytic conditions, and it is difficult to obtain preparative quantities of the compounds by gas phase synthesis. Many stable heterometallic complexes that contain Au–H–M bonds<sup>15</sup> (M ≠ Au) were also synthesized on a preparative scale. However, these complexes are not suitable as models for gold hydride catalysis. Synthesis of a simple monomeric gold(I) hydride complex (HAuL, L: ligand) had been desired for a long time. Very recently, Tsui and co-workers reported the first synthesis of a monomeric gold(I) hydride complex, utilizing

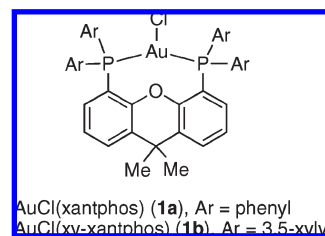


**Figure 1.** AuCl(xantphos) (**1a**) and AuCl(xy-xantphos) (**1b**) complexes.

an N-heterocyclic carbene (NHC) ligand, IPr (IPr = 1,3-bis(2,6-diisopropylphenyl)imidazol-2-ylidene), as the supporting ligand that stabilized the gold(I) hydride structure.<sup>16</sup> This compound is stable against exposure to air and moisture in the solid state but is decomposed slowly in solution. Although stoichiometric reactions of the gold(I) hydride with dimethyl acetylenedicarboxylate and ethyl diazoacetate were reported, catalytic properties of this complex were not described in the paper.<sup>16</sup>

We recently reported gold(I)-catalyzed dehydrogenative silylation of alcohols with hydrosilanes, in which a gold(I) hydride intermediate was proposed as a key species, despite the fact that spectroscopic evidence for the formation of the gold(I) hydride intermediate was not shown.<sup>6a</sup> Dehydrogenative silylation of alcohols is a more selective and environmentally benign process for producing silyl ethers than conventional chlorosilane/base silylation.<sup>17</sup> A number of transition-metal complexes exhibit catalytic activity in dehydrogenative silylation of alcohols, although they often suffer from low functional group compatibility. This is thought to be because such complexes typically have catalytic activity for undesired hydrosilylation of the unsaturated functionalities in the substrates. An interesting feature of the AuCl(xantphos)-catalyzed reaction is that it tolerates a wide range of functional groups including alkenes, alkynes, alkyl halides (RCl, RBr), ketones, aldehydes, conjugated enones, esters, and carbamates. Furthermore, this reaction can be carried out in numerous solvents (Scheme 1). In addition to these unique chemoselectivities, it is also noteworthy that the catalytic activity strongly depends on the phosphine ligand of the gold(I) catalyst. Of the various combinations of phosphine ligands and gold(I) salts, only the Xantphos ligand showed reasonable catalytic activity for this gold(I)-catalyzed dehydrogenative silylation.<sup>6,18</sup> In an effort to understand these characteristic features of the AuCl(xantphos)-catalyzed reaction as well as design new gold(I)

(7) For gold-catalyzed hydroboration, see: Baker, R. T.; Calabrese, J. C.; Westcott, S. A. *J. Organomet. Chem.* **1995**, 498, 109–117.

(8) For C–H activation reactions, see: (a) Wei, C.; Li, C.-J. *J. Am. Chem. Soc.* **2003**, 125, 9584–9585. (b) Skouta, R.; Li, C.-J. *Angew. Chem., Int. Ed.* **2007**, 46, 1117–1119. (c) Zhang, X.; Corma, A. *Angew. Chem., Int. Ed.* **2008**, 47, 4358–4361.

(9) For examples of gold-catalyzed aerobic oxidations of alcohols, see: (a) Abad, A.; Almela, C.; Corma, A.; García, H. *Chem. Commun.* **2006**, 3178–3180. (b) Abad, A.; Corma, A.; García, H. *Chem.—Eur. J.* **2008**, 14, 212–222. (c) Conte, M.; Miyamura, H.; Kobayashi, S.; Chechik, V. J. *Am. Chem. Soc.* **2009**, 131, 7189–7196.

(10) For dehydrogenative dimerization of trialkylstananes, see: Ito, H.; Yajima, T.; Tateiwa, J.; Hosomi, A. *Tetrahedron Lett.* **1999**, 40, 7807–7810.

(11) For reviews of gold hydride compounds, see: (a) Puddephatt, R. J. In *Comprehensive Coordination Chemistry: The Synthesis, Reactions, Properties & Applications of Coordination Compounds*; Wilkinson, G., Gillard, R. D., McCleverty, J. A., Eds.; Pergamon Press: Oxford, 1987; Vol. 5, p 869. (b) Crawford, M. J.; Klapotke, T. M. *Angew. Chem., Int. Ed.* **2002**, 41, 2269–2271. (c) Gimeno, M. C.; Laguna, A. In *Comprehensive Coordination Chemistry II: From Biology to Nanotechnology*; McCleverty, J. A., Meyer, T. B., Eds.; Elsevier: Oxford, 2004; Vol. 6, pp 1073–1075.

(12) For reviews of theoretical studies on gold hydrides, see: (a) Pyykkö, P. *Angew. Chem., Int. Ed.* **2004**, 43, 4412–4456. (b) Pyykkö, P. *Inorg. Chim. Acta* **2005**, 358, 4113–4130. (c) Pyykkö, P. *Chem. Soc. Rev.* **2008**, 37, 1967–1997.

(13) For the matrix isolation and the characterization of AuH, AuH<sub>n</sub>, and AuH<sub>n</sub>(H<sub>2</sub>) compounds, see: (a) Ringström, U. *Nature* **1963**, 198, 981. (b) Wang, X. F.; Andrews, L. *J. Am. Chem. Soc.* **2001**, 123, 12899–12900. (c) Wang, X. F.; Andrews, L. *J. Phys. Chem. A* **2002**, 106, 3744–3748. (d) Andrews, L. *Chem. Soc. Rev.* **2004**, 33, 123–132.

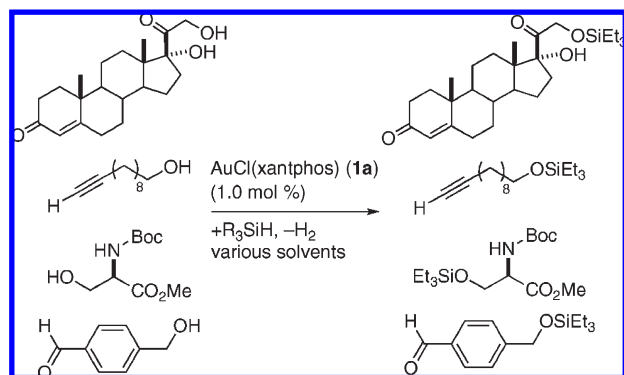
(14) For gas phase synthesis of Au<sub>n</sub>H<sup>+</sup> and Au<sub>n</sub>H<sup>−</sup> type compounds, see: (a) Fischer, D.; Wanda, A.; Curioni, A.; Grönbeck, H.; Burkart, S.; Ganteför, G. *Chem. Phys. Lett.* **2002**, 361, 389–396. (b) Buckart, S.; Ganteför, G.; Kim, Y. D.; Jena, P. *J. Am. Chem. Soc.* **2003**, 125, 14205–14209. (c) Sugawara, K.; Sobott, F.; Vakhtin, A. B. *J. Chem. Phys.* **2003**, 118, 7808–7816. (d) Zhai, H.; Kiran, B.; Wang, L. *J. Chem. Phys.* **2004**, 121, 8231–8236. (e) Khairallah, G.; O'hair, R.; Bruce, M. *Dalton. Trans.* **2006**, 3699–3707.

(15) For examples of heterometallic compounds containing Au–H–M (M ≠ Au) moieties, see: (a) Lehner, H.; Matt, D.; Pregosin, P. S.; Venanzi, L. M.; Albinati, A. *J. Am. Chem. Soc.* **1982**, 104, 6825–6827. (b) Casalnuovo, A. L.; Pignolet, L. H.; van der Velden, J. W. A.; Bour, J. J.; Steggerda, J. J. *J. Am. Chem. Soc.* **1983**, 105, 5957–5958. (c) Alexander, B. D.; Johnson, B. J.; Johnson, S. M.; Casalnuovo, A. L.; Pignolet, L. H. *J. Am. Chem. Soc.* **1986**, 108, 4409–4417. (d) Albinati, A.; Lehner, H.; Venanzi, L. M.; Wolfer, M. *Inorg. Chem.* **1987**, 26, 3933–3939. (e) Albinati, A.; Chaloupka, S.; Currao, A.; Klooster, W. T.; Koetzle, T. F.; Nesper, R.; Venanzi, L. M. *Inorg. Chim. Acta* **2000**, 300–302, 903–911.

(16) Tsui, E.; Müller, P.; Sadighi, J. R. *Angew. Chem., Int. Ed.* **2008**, 47, 8937–8940.

(17) For selected examples of dehydrogenative alcohol silylation, see: (a) Lukevics, E.; Dzintara, M. *J. Organomet. Chem.* **1985**, 295, 265–315. (b) Luo, X. L.; Crabtree, R. H. *J. Am. Chem. Soc.* **1989**, 111, 2527–2535. (c) Tanabe, Y.; Okumura, H.; Maeda, A.; Murakami, M. *Tetrahedron Lett.* **1994**, 35, 8413–8414. (d) Lorenz, C.; Schubert, U. *Chem. Ber.* **1995**, 128, 1267–1269. (e) Blackwell, J. M.; Foster, K. L.; Beck, V. H.; Piers, W. E. *J. Org. Chem.* **1999**, 64, 4887–4892. (f) Chung, M. K.; Orlova, G.; Goddard, J. D.; Schlaf, M.; Harris, R.; Beveridge, T. J.; White, G.; Hallett, F. R. *J. Am. Chem. Soc.* **2002**, 124, 10508–10518. (g) Field, L. D.; Messerle, B. A.; Rehr, M.; Soler, L. P.; Hambley, T. W. *Organometallics* **2003**, 22, 2387–2395. (h) Schmidt, D. R.; O'Malley, S. J.; Leighton, J. L. *J. Am. Chem. Soc.* **2003**, 125, 1190–1191. (i) Biffis, A.; Braga, M.; Basato, M. *Adv. Synth. Catal.* **2004**, 346, 451–458. (j) Rendler, S.; Auer, G.; Oestreich, M. *Angew. Chem., Int. Ed.* **2005**, 44, 7620–7624. (k) Wile, B. M.; McDonald, R.; Ferguson, M. J.; Stradiotto, M. *Organometallics* **2007**, 26, 1069–1076. (l) Hara, K.; Akiyama, R.; Takakusagi, S.; Uosaki, K.; Yoshino, T.; Kagi, H.; Sawamura, M. *Angew. Chem., Int. Ed.* **2008**, 47, 5627–5630.



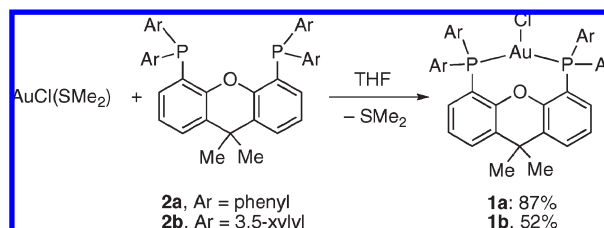
**Scheme 1. Gold(I)-Catalyzed Dehydrogenative Alcohol Silylation**

hydride-mediated catalysts, it is desirable to study the structure and reactivities of the key gold(I) hydride intermediates.

Herein, we report the first study on gold(I) hydride in terms of the synthesis, spectroscopic characterization, and reaction behavior in the catalysis. We found that the gold(I) hydride species can be generated by the reaction between gold(I) chloride complexes and hydrosilanes. The characterization was carried out by  $^1\text{H}$ ,  $^2\text{H}$ , and  $^{31}\text{P}$  NMR measurements and ESI mass spectrometry. We also demonstrated that the gold(I) hydride complex is an active intermediate in the dehydrogenative alcohol silylation by in situ NMR monitoring experiments. High stability of the chelating P–Au–P motifs of gold(I)/Xantphos or gold(I)/xy-Xantphos and the high reactivity induced by the chelating structure are responsible for their outstanding high catalytic activity. A modified reaction mechanism involving the acid-mediated chlorination of gold(I) hydride species was proposed on the basis of spectroscopic and kinetic experiments.

## Results and Discussion

**Synthesis and Characterization of AuCl(xantphos) (1a) and AuCl(xy-xantphos) (1b).** Tricoordinated chlorogold(I)–diphosphine complexes AuCl(xantphos) (**1a**) and AuCl(xy-xantphos) (**1b**) were prepared as previously described<sup>16a,18a,19</sup> and are shown in Scheme 2. Although tricoordinated, monomeric gold(I) complexes are rare species,<sup>20</sup> **1a** and **1b** can be formed only by simply mixing AuCl(SMe<sub>2</sub>) with 1.0 equiv of Xantphos (**2a**) or xy-Xantphos (4,5-bis[bis(3,5-dimethylphenyl)phosphino]-9,9-dimethylxanthene) (**2b**) in THF. Although

**Scheme 2. Synthesis of Gold(I) Complexes 1a and 1b**

**1a** was observed as the major product, small amounts of digold complex  $[(\text{AuCl})_2\text{xantphos}]^{20b}$  and cationic tetracoordinated complex  $[\text{Au}(\text{xantphos})_2]\text{X}$  ( $\text{X} = \text{Cl}^-$ ,  $\text{AuCl}_2^-$ )<sup>20b</sup> were also detected in the reaction mixture of **2a** and AuCl(SMe<sub>2</sub>). After evaporation, recrystallization of the residue from hot benzonitrile afforded pure AuCl(xantphos) (**1a**) as inclusion crystals with benzonitrile. In order to remove benzonitrile, precipitation from a chloroform solution of the inclusion crystals by the addition of hexane was carried out, affording **1a** as a white powder in high yield (87%). The thus obtained air- and moisture-stable compound can be stored for several months in the solid state without degradation. In CDCl<sub>3</sub>, **1a** is stable for at least one day. However, in CH<sub>2</sub>Cl<sub>2</sub>, partial disproportionation from **1a** to  $[(\text{AuCl})_2\text{xantphos}]$  and  $[\text{Au}(\text{xantphos})_2]\text{X}$  ( $\text{X} = \text{Cl}^-$ ,  $\text{AuCl}_2^-$ ) was observed immediately after dissolution of **1a**.<sup>20b</sup> AuCl(xy-xantphos) (**1b**) is more stable in solution than **1a** and could be isolated by column chromatography (SiO<sub>2</sub>, CHCl<sub>3</sub>/MeOH, 97:3) with a good yield (52%). The disproportionation of **1b** was not detected for any of the solvents tested.

Complexes **1a** and **1b** were characterized by  $^1\text{H}$ ,  $^{13}\text{C}$ , and  $^{31}\text{P}\{^1\text{H}\}$  NMR spectroscopy, as well as mass spectrometry (see Supporting Information). Single sets of resonances were observed in the  $^1\text{H}$ ,  $^{13}\text{C}$ , and  $^{31}\text{P}\{^1\text{H}\}$  NMR spectra of both **1a** and **1b** in CDCl<sub>3</sub>. The  $^1\text{H}$  NMR shifts of the CDCl<sub>3</sub> solutions of both **1a** and **1b** in the aromatic region show downfield shifts ( $\Delta\delta$  0.05–0.30) relative to free ligands **2a** and **2b**. Single sharp peaks were observed in the  $^{31}\text{P}\{^1\text{H}\}$  NMR spectra of **1a** and **1b**. Coordination to the gold(I) center produced a significant downfield shift of the coordinating phosphorus atoms at  $\delta$  –17.5 (**2a**) and –16.8 (**2b**) to 28.8 (**1a**) and 28.6 (**1b**), respectively. APCI-HRMS analysis of **1a** and **1b** showed peaks for the dechlorinated cations of **1a** ( $[\text{1a} - \text{Cl}]^+$ , calcd 775.1594, found 775.1568) and **1b** ( $[\text{1b} - \text{Cl}]^+$ , calcd 887.2856, found 887.2871). The spectral data support the tricoordinated, monomeric structures of **1a** and **1b** in solution.

The tricoordinated, monomeric structures of **1a** and **1b** were confirmed by X-ray crystallographic analysis (Figure 2). Single crystals of both complexes were prepared by recrystallization from hexane/benzene. The crystals of **1a** were obtained as a hemibenzenate (**1a**·(C<sub>6</sub>H<sub>6</sub>)<sub>1.5</sub>). The crystals of **1b** contain two different conformational isomers in the crystal structure without solvent inclusion. The essential molecular structures of **1a** and **1b** are very similar. The complexes have tricoordinated geometry around the gold atoms coordinated by the Xantphos (**2a**) or xy-Xantphos (**2b**) ligand with P–Au–P angles of 116.7° (**1a**) and 117.8° and 120.6° (**1b**) (Table 1). These angles are much smaller than that of AuCl(PPh<sub>3</sub>)<sub>2</sub> (**1c**)<sup>21b</sup> (135.7°), which was reported to have a tricoordinated structure in the solid state. In **1a** and **1b**, Au, P, and Cl atoms lie in the same plane, as indicated by the sum of the P–Au–P, P–Au–Cl, and Cl–Au–P angles (359.9° (**1a**), 360.0 and 359.9 (**1b**)). The long atomic distances between gold and oxygen atoms in the crystal structures

(18) For our recent studies on catalytic reactions with copper(I)–Xantphos complexes, see: (a) Ito, H.; Watanabe, A.; Sawamura, M. *Org. Lett.* **2005**, *7*, 1869–1871. (b) Ito, H.; Kawakami, C.; Sawamura, M. *J. Am. Chem. Soc.* **2005**, *127*, 16034–16035. (c) Ito, H.; Ito, S.; Sasaki, Y.; Matsuura, K.; Sawamura, M. *J. Am. Chem. Soc.* **2007**, *129*, 14856–14857. (d) Ito, H.; Kosaka, Y.; Nonoyama, K.; Sasaki, Y.; Sawamura, M. *Angew. Chem., Int. Ed.* **2008**, *47*, 7424–7427. (e) Ito, H.; Sasaki, Y.; Sawamura, M. *J. Am. Chem. Soc.* **2008**, *130*, 15774–15776.

(19) Kranenburg, M.; van der Burgt, Y. E. M.; Kamer, P. C. J.; van Leeuwen, P. W. N. M.; Goubitz, K.; Fraanje, J. *Organometallics* **1995**, *14*, 3081–3089.

(20) For Au(I)/xantphos complexes, see: (a) Pawlowski, V.; Kunkely, H.; Vogler, A. *Inorg. Chim. Acta* **2004**, *357*, 1309–1312. (b) Pintado-Alba, A.; de la Riva, H.; Nieuwhuyzen, M.; Bautista, D.; Raithby, P. R.; Sparkes, H. A.; Teat, S. J.; López-de-Luzuriaga, J. M.; Lagunas, M. C. *Dalton Trans* **2004**, 3459–3467. (c) Deák, A.; Megyes, T.; Tárkányi, G.; Király, P.; Biczók, L.; Pálincás, G.; Stang, P. J. *J. Am. Chem. Soc.* **2006**, *128*, 12668–12670. (d) Lagunas, M. C.; Fierro, C. M.; Pintado-Alba, A.; de la Riva, H.; Betanzos-Lara, S. *Gold Bull.* **2007**, *40*, 135–141. (e) Zsila, F.; Bikadi, Z.; Hazai, E.; Simon, A.; Fitos, I.; Mady, G. *Biochim. Biophys. Acta, Proteins Proteomics* **2008**, *1784*, 1106–1114.

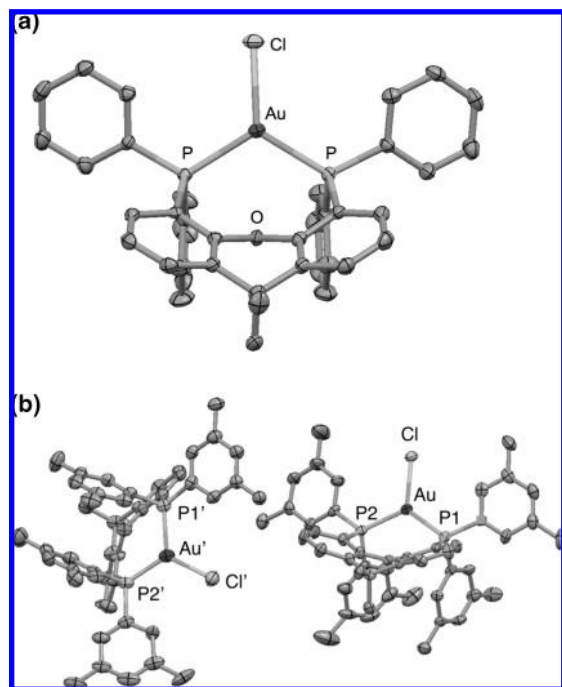


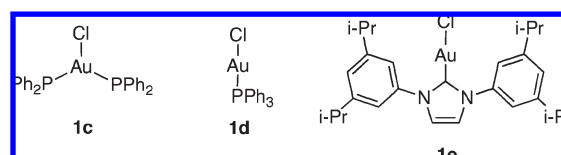
**Figure 2.** (a) ORTEP diagram of AuCl(xantphos) (**1a**) with 50% ellipsoids. Hydrogen atoms and solvent molecules are omitted for clarity. (b) ORTEP diagram of AuCl(xy-xantphos) (**1b**) in two different conformations in the crystal structure with 50% ellipsoids. Hydrogen atoms are omitted for clarity.

suggest that the oxygen atoms do not coordinate to the gold atoms (Au $\cdots$ O: 3.203 Å (**1a**), 3.173, 3.124 Å (**1b**)).

The Au–Cl bonds of **1a** (2.462 Å) and **1b** (2.457, 2.475 Å) are much longer than that of monophosphine complex AuCl(PPh<sub>3</sub>) (**1d**) (2.279 Å).<sup>21a</sup> The long bond lengths for **1a** and **1b** indicate activation of the Au–Cl bonds by the formation of the stable tricoordinated complexes with Xantphos and xy-Xantphos. AuCl(PPh<sub>3</sub>)<sub>2</sub> (**1c**) was reported to have a slightly longer Au–Cl bond (2.533 Å) than that for **1a** (2.462 Å) and **1b** (2.457 and 2.475 Å). The Au–Cl bond length (2.270 Å) of [AuCl(IPr)]<sup>21c</sup> (**1e**, IPr = 1,3-bis-(diisopropylphenyl)imidazol-2-ylidene), which is the supporting ligand for the stable gold(I) hydride complex reported by Tsui and co-workers,<sup>16</sup> is similar to that of monotriphenylphosphine complex AuCl(PPh<sub>3</sub>) (**1d**) (2.279 Å), indicating that activation of the IPr ligand on the Au–Cl bond is not significant compared to those for **1a** and **1b**.<sup>22</sup>

**Ligand Effect in Gold(I)-Catalyzed Dehydrogenative Silylation of Alcohols.** In an effort to examine the ligand effect in the gold(I)-catalyzed dehydrogenative alcohol silylation, various phosphines were subjected to the catalytic reaction (Table 2). Only gold(I) catalysts with the Xantphos and xy-

**Table 1.** Selected X-ray Structural Data for **1a–e**



	<b>1a</b> (C <sub>6</sub> H <sub>6</sub> ) <sub>1.5</sub>	<b>1b</b>	<b>1c</b> <sup>a</sup>	<b>1d</b> <sup>a</sup>	<b>1e</b> <sup>a</sup>
Bond Lengths (Å)					
Au–Cl	2.4620(9)	2.457(3), 2.475(2)	2.533(4)	2.279(3)	2.270(1)
P1–Au	2.3330(8)	2.338(2), 2.336(2)	2.316(4)	2.235(4)	
P2–Au	2.3488(8)	2.317(3), 2.335(2)	2.336(4)		
Bond Angles (deg)					
P1–Au–P2	116.73(3)	117.81(9), 120.61(7)	135.7(1)		

<sup>a</sup> Data were taken from the literature.<sup>21</sup>

Xantphos ligands showed high activity among the gold(I)/phosphine complexes tested. The gold(I) catalysts were prepared by mixing AuCl(SMe<sub>2</sub>) and a phosphine ligand, followed by removal of free SMe<sub>2</sub> in vacuo. The catalytic activities of the gold(I) complexes were determined from the yield of a silyl ether (**5a**) after reaction of 2-phenylethanol (**3a**) with HSiEt<sub>3</sub> (**4a**) in 1,2-dichloroethane at 50 °C for 2.5 h in the presence of 1 mol % gold(I) catalyst.

The use of AuCl(SMe<sub>2</sub>) without addition of a phosphine ligand resulted in a poor yield (11%) of **3a**, accompanied by precipitation of metallic gold in the early stage of the reaction (within 10 min) (entry 1). The Xantphos ligand performed significantly better than the other phosphine ligands including the monodentate (PPh<sub>3</sub>) and bidentate phosphines (dppe, dppp, dppb, dppf, DPEphos,<sup>19</sup> and DBFphos<sup>19</sup>), producing the silyl ether in 94% yield without side products or precipitation of metallic gold; the other ligands produced a yield of less than 11% (entries 2–9). Isolated AuCl(PPh<sub>3</sub>)<sub>2</sub> (**1c**) gave a low yield (2%) under identical conditions (entry 10). The isolated AuCl(xantphos) (**1a**) complex was slightly more active than the catalyst generated *in situ* (entry 11, 100%, 2 h). AuCl(xy-xantphos) (**1b**) showed the highest catalytic activity. Reaction with **1b** was complete after a shorter time than that with **1a** (entry 12, 100%, 1.5 h).<sup>23</sup> In reactions with **1a** and **1b**, the reaction mixtures were colorless or pale pink until the alcohol was consumed. After the alcohol was consumed, the reaction mixture turned burgundy red.

The high activities of AuCl(xantphos) (**1a**) and AuCl(xy-xantphos) (**1b**) may be partially attributed to the ability to keep monomeric tricoordinated structures around the gold(I) center in solution. Complexes of Au(I)X (X = Cl, Br, I, CN, etc.) with phosphine ligands generally tend to form linear dicoordinated complexes (X–Au–PR<sub>3</sub>).<sup>20,21,24,25</sup>

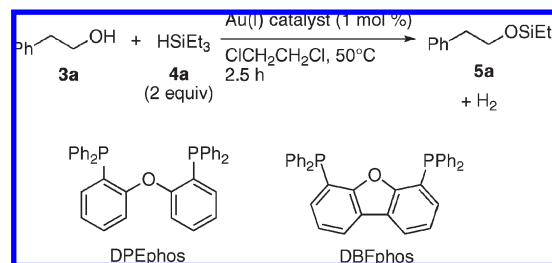
(21) For X-ray structure of gold(I) complexes: (a) Baenziger, N. C.; Bennett, W. E.; Soborof, D. M. *Acta Crystallogr., Sect. B* **1976**, 32, 962–963. (b) Bowmaker, G. A.; Dyason, J. C.; Healy, P. C.; Engelhardt, L. M.; Pakawatchai, C.; White, A. H. *J. Chem. Soc., Dalton Trans.* **1987**, 1089–1097. (c) Frutos, M. R.; Belderrain, T. R.; Frémont, P.; Scott, N. M.; Nolan, S. P.; Dkz-Requejo, M. M.; Pérez, P. J. *Angew. Chem., Int. Ed.* **2005**, 44, 5284–5288. (d) Herrero-Gómez, E.; Nieto-Oberhuber, C.; López, S.; Benet-Buchholz, J.; Echavarren, A. M. *Angew. Chem., Int. Ed.* **2006**, 45, 5455–5459. (e) Partyka, D. V.; Robilotto, T. J.; Zeller, M.; Hunter, A. D.; Gray, T. G. *Organometallics* **2008**, 27, 28–32.

(22) For electronic properties of NHC ligands, see: (a) Dorta, R.; Stevens, E. D.; Scott, N. M.; Costabile, C.; Cavallo, L.; Hoff, C. D.; Nolan, S. P. *J. Am. Chem. Soc.* **2005**, 127, 2485–2495. (b) Dkz-González, S.; Nolan, S. P. *Coord. Chem. Rev.* **2007**, 251, 874–883.

(23) Substitution at the *meta*-position of the phenyl rings on phosphorous atoms in the xy-Xantphos ligand is thought to be important for the high activity. Use of tol-Xantphos {4,5-bis[bis(4-methylphenyl)phosphino]-9,9-dimethylxanthene} instead of xy-Xantphos as the ligand resulted in lower activity.

(24) For structures of AuCl/diphosphine complexes in solution, see: (a) Berners-Price, S. J.; Mazid, M. A.; Sadler, P. J. *J. Chem. Soc., Dalton Trans.* **1984**, 969–974. (b) Berners-Price, S. J.; Sadler, P. J. *Inorg. Chem.* **1986**, 25, 3822–3827. (c) Berners-Price, S. J.; Bowen, R. J.; Hambley, T. W.; Healy, P. C. *J. Chem. Soc., Dalton Trans.* **1999**, 1337–1346.

(25) For a review of three-coordinated gold complexes, see: Carvajal, M. A.; Novoa, J. J.; Alvarez, S. *J. Am. Chem. Soc.* **2004**, 126, 1465–1477.

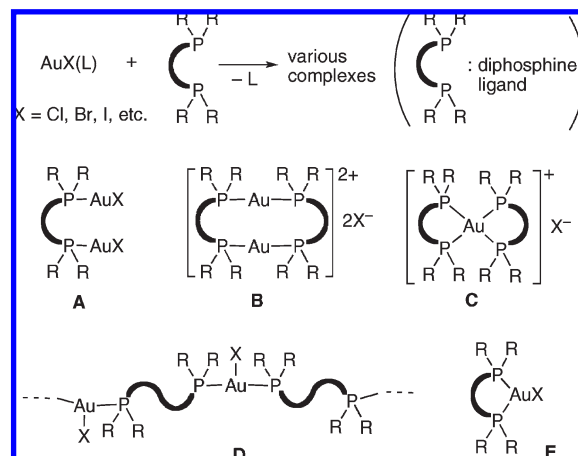
**Table 2. Ligand Effect in Au(I)-Catalyzed Dehydrogenative Silylation<sup>a</sup>**

entry	catalyst	yield (%) <sup>b</sup>
1	$\text{AuCl}(\text{SMe}_2)$	11
2	Xantphos/ $\text{AuCl}(\text{SMe}_2)$	94
3	$\text{PPh}_3$ / $\text{AuCl}(\text{SMe}_2)$	trace
4	dppe/ $\text{AuCl}(\text{SMe}_2)$	0
5	dppp/ $\text{AuCl}(\text{SMe}_2)$	trace
6	dppb/ $\text{AuCl}(\text{SMe}_2)$	trace
7	dppf/ $\text{AuCl}(\text{SMe}_2)$	11
8	DPEphos/ $\text{AuCl}(\text{SMe}_2)$	5
9	DBFphos/ $\text{AuCl}(\text{SMe}_2)$	0
10 <sup>c</sup>	$\text{AuCl}(\text{PPh}_3)_2$ ( <b>1c</b> )	2
11 <sup>c,d</sup>	$\text{AuCl}(\text{xantphos})$ ( <b>1a</b> )	100
12 <sup>c,e</sup>	$\text{AuCl}(\text{xy-xantphos})$ ( <b>1b</b> )	100

<sup>a</sup> Conditions:  $\text{AuCl}(\text{SMe}_2)$  (1.0 mol %, 0.005 mmol), ligand (1.0 mol %, 0.005 mmol) with an alcohol **3** (0.5 mmol) and hydrosilane **4** (1.0 mmol) in 1,2-dichloroethane (0.5 mL) at  $50^\circ\text{C}$ . <sup>b</sup> GC yield of the silyl ether. No side reaction occurred. <sup>c</sup> Isolated complex was used. <sup>d</sup> Yield after reaction for 2 h. <sup>e</sup> Yield after reaction for 1.5 h.

Monomeric tricoordinated complexes  $\text{XAu}(\text{PR}_3)_2$  are thought to be less stable than dicoordinated complexes and, in fact, rarely occur when diphosphine ligands are used.<sup>26</sup> As is illustrated in Figure 3,<sup>7,24</sup> coordination of ordinary diphosphine ligands to  $\text{Au}(\text{I})\text{X}$  resulted in mixtures of various coordination structures such as dicoordinated digold complexes (**A**) and dimeric complexes (**B**). In some cases, tetracoordinated cationic complexes (**C**) and polymeric structures (**D**) were observed. Only a limited number of tricoordinated monomeric complexes (**E**) have been reported.<sup>26</sup>

In order to compare the coordination behavior of the  $\text{AuCl}$ /phosphine complexes under conditions similar to those for catalytic reactions, the  $^{31}\text{P}\{^1\text{H}\}$  NMR measurements of mixtures of  $\text{AuCl}(\text{SMe}_2)$  and phosphines [ $\text{PPh}_3$  (1 and 2 equiv), dppe, dppp, dppb, dppf, DPEphos, and DBFphos] in  $\text{CDCl}_3$  were conducted at  $20^\circ\text{C}$  with 1:1 or 1:2 molar ratios of gold(I) to phosphine (Figure 4).<sup>27</sup>  $\text{AuCl}(\text{xantphos})$  (**1a**),  $\text{AuCl}(\text{xy-xantphos})$  (**1b**), and the 1:1 mixture of  $\text{AuCl}$  and  $\text{PPh}_3$  show single sharp resonances

**Figure 3.** Various structures of complexes formed by mixing a gold(I) salt and a diphosphine ligand.

(Figures 4a–c), although all other solutions of  $\text{AuCl}$ /phosphine resulted in multiple and broad resonances, consistent with the results of previous studies (Figures 4d–j).<sup>24</sup> The broad resonance for the mixture of  $\text{AuCl}(\text{SMe}_2)$  and 2 equiv of  $\text{PPh}_3$  could be attributed to disproportionation of the tricoordinated  $\text{AuCl}(\text{PPh}_3)_2$  (**1c**) into dicoordinated  $\text{AuCl}(\text{PPh}_3)$  (**1d**) and tetracoordinated  $\text{AuCl}(\text{PPh}_3)_3$  (Figure 4d).<sup>28</sup> The equilibrium for several coordination structures may be responsible for the multiple broad resonances observed for solutions of  $\text{AuCl}$ /phosphine (Figure 4e–j). Both  $\text{AuCl}(\text{xantphos})$  (**1a**) and  $\text{AuCl}(\text{xy-xantphos})$  (**1b**) are tricoordinated in the monomeric form. In these structures, the  $\text{Au}–\text{Cl}$  bonds are activated by chelation.<sup>29</sup> The gold(I) complexes, with the exception of those for **1a** and **1b**, did not react with hydrosilanes. No significant changes in the  $^{31}\text{P}\{^1\text{H}\}$  NMR spectra were observed after addition of  $\text{PhMe}_2\text{SiH}$  (**4b**) to the solutions of the  $\text{AuCl}$ /phosphine mixture, except in the cases of **1a** and **1b**.

**Synthesis and Characterization of Gold(I) Hydride Complexes.** A gold(I) hydride species (**6b**) was generated from  $\text{AuCl}(\text{xy-xantphos})$  (**1b**) by reaction with hydrosilane **4b** in  $\text{CDCl}_3$  (Scheme 3). To a  $\text{CDCl}_3$  solution (0.5 mL) of  $\text{AuCl}(\text{xy-xantphos})$  (**1b**) (25.0 mg, 0.027 mmol) in an NMR sample tube under argon was added 2 equiv of  $\text{PhMe}_2\text{SiH}$  (**4b**) (7.5 mg, 0.055 mmol) at room temperature in the dark. The starting complex **1b** was converted to the new complex **6b** in good yield (79%) within 30 min. A quantity of 0.5 equiv of  $\text{PhMe}_2\text{SiCl}$  (**7b**) (47%, based on **1b**) also formed. This new gold(I) hydride complex (**6b**) was stable for one day in the dark, although removal of the solvent by evaporation or precipitation into hexane led to partial decomposition of **6b** into **1b**. **6b** is not very sensitive to light, but partial decomposition of **6b** was observed after exposure to room light in the NMR sample tube for a few hours. Accordingly, the characterization of **6b** with NMR spectroscopy was carried out in solution in the dark.

(26) For monomeric three-coordinated  $\text{AuX}$ –diphosphine complexes, see: (a) Barrow, M.; Bürgi, H. B.; Johnson, D. K.; Venanzi, L. M. *J. Am. Chem. Soc.* **1976**, *98*, 2356–2357. (b) Crespo, O.; Gimeno, M. C.; Laguna, A.; Jones, P. G. *J. Chem. Soc., Dalton Trans.* **1992**, 1601–1605. (c) Viotte, M.; Gautheron, B.; Kubicki, M. M.; Mugnier, Y.; Parish, R. V. *Inorg. Chem.* **1995**, *34*, 3465–3473. (d) Cooke, P. A.; Perera, S. D.; Shaw, B. L.; Thornton-Pett, M.; Vessey, J. D. *J. Chem. Soc., Dalton Trans.* **1997**, 435–438. (e) Sterzik, A.; Rys, E.; Blaurock, S.; Hey-Hawkins, E. *Polyhedron* **2001**, *20*, 3007–3014. (f) Eisler, D. J.; Puddephatt, R. J. *Inorg. Chem.* **2003**, *42*, 6352–6365. (g) Xu, F. B.; Li, Q. S.; Wu, L. Z.; Leng, X. B.; Li, Z. C.; Zeng, X. S.; Chow, Y. L.; Zhang, Z. Z. *Organometallics* **2003**, *22*, 633–640.

(27) A  $\text{CDCl}_3$  solution of the phosphine (0.01 mmol, 1.0 mL) was added to  $\text{AuCl}(\text{SMe}_2)$  (0.01 mmol) with stirring under air. After 30 min, the volatile compounds were removed in vacuo. The resultant solid was subjected to NMR measurements after dissolution in  $\text{CDCl}_3$  (1.0 mL).

(28) For disproportionation of  $\text{AuCl}(\text{PPh}_3)_2$  in solution, see: (a) Muetterties, E. L.; Alegranti, C. W. *J. Am. Chem. Soc.* **1970**, *92*, 4114–4115. (b) Baenziger, N. C.; Dittmore, K. M.; Doyle, J. R. *Inorg. Chem.* **1974**, *13*, 805–811.

(29) Bürgi and co-workers discussed the elongation of the  $\text{Au}–\text{Cl}$  bond in  $\text{AuCl}(\text{transphos})$  [transphos: 2,11-bis(diphenylphosphino)methylbenzo[*c*]phenanthrene], see ref 26a. See also: DeStefano, N. J.; Johnson, D. K.; Lane, R. M.; Venanzi, L. M. *Helv. Chim. Acta* **1976**, *59*, 2674–2682.



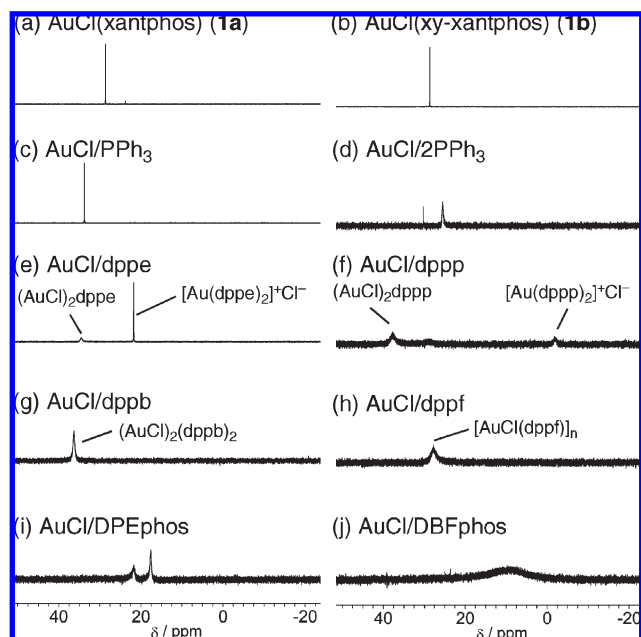
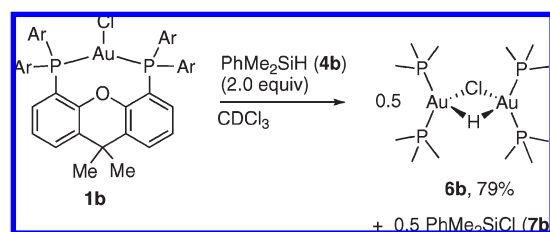


**Figure 4.**  $^{31}\text{P}\{^1\text{H}\}$  NMR spectra for (a)  $\text{AuCl}(\text{xantphos})$  (**1a**), (b)  $\text{AuCl}(\text{xy-xantphos})$  (**1b**), and mixtures of  $\text{AuCl}(\text{SMe}_2)$  and a phosphine: (c)  $\text{PPh}_3$ , (d)  $\text{PPh}_3$  (2.0 equiv), (e)  $\text{dppe}$ , (f)  $\text{dppp}$ , (g)  $\text{dppb}$ , (h)  $\text{dppf}$ , (i)  $\text{DPEphos}$ , and (j)  $\text{DBFphos}$ . All measurements were conducted at a concentration of 0.01 mol/L (for gold(I) atom) in  $\text{CDCl}_3$  at  $20^\circ\text{C}$ .

### Scheme 3. Generation of Gold(I) Hydride Complex **6b**



In the  $^1\text{H}$  NMR spectrum, a characteristic signal, which was assigned to the desirable hydride ligand, was observed at  $\delta = 8.29$  ppm as a quintet ( $^2J_{\text{H,P}} = 49.5$  Hz) (Figure 5b). The resonances for **6b** in the aromatic region were overlapped by the resonances for **4b** and **7b**. Therefore, the compound was fully characterized by the  $^1\text{H}$  NMR spectrum obtained by the reaction with  $\text{C}_6\text{D}_5\text{Me}_2\text{SiH}$  (**4c**) rather than **4b** (Figure 5c). In the  $^{31}\text{P}\{^1\text{H}\}$  NMR spectrum for **6b**, a singlet for gold(I) precursor **1b** at 28.7 ppm almost completely disappeared and a new singlet appeared at 33.8 ppm (Figure 6a and b). In the  $^{31}\text{P}$  NMR spectrum obtained without broadband decoupling of the hydrogen atoms, a resonance at 33.8 ppm was observed as a broad doublet ( $^2J_{\text{P,H}} = 49.6$  Hz) (Figure 6b). The HETCOR(H/P) spectrum showed an apparent cross-peak between the ligand phosphorus atoms and the hydride ligand (see Supporting Information). On the basis of the coupling pattern and integrals of the hydride resonance (0.5 H, based on the ligand protons), it is obvious that gold(I) hydride **6b** has a  $\text{P}_2\text{Au}-\text{H}-\text{AuP}_2$  motif with four symmetrically equivalent phosphorus atoms.<sup>30</sup>

(30) A triplet for H–D ( $\sigma = 4.56$  ppm,  $J_{\text{H,D}} = 48.6$  Hz) was observed in the  $^1\text{H}$  NMR spectrum after the addition of methanol- $d_4$  to the reaction mixture of **1b** and a hydrosilane or the addition of methanol to the reaction mixture of **1b** and a deuteriosilane.

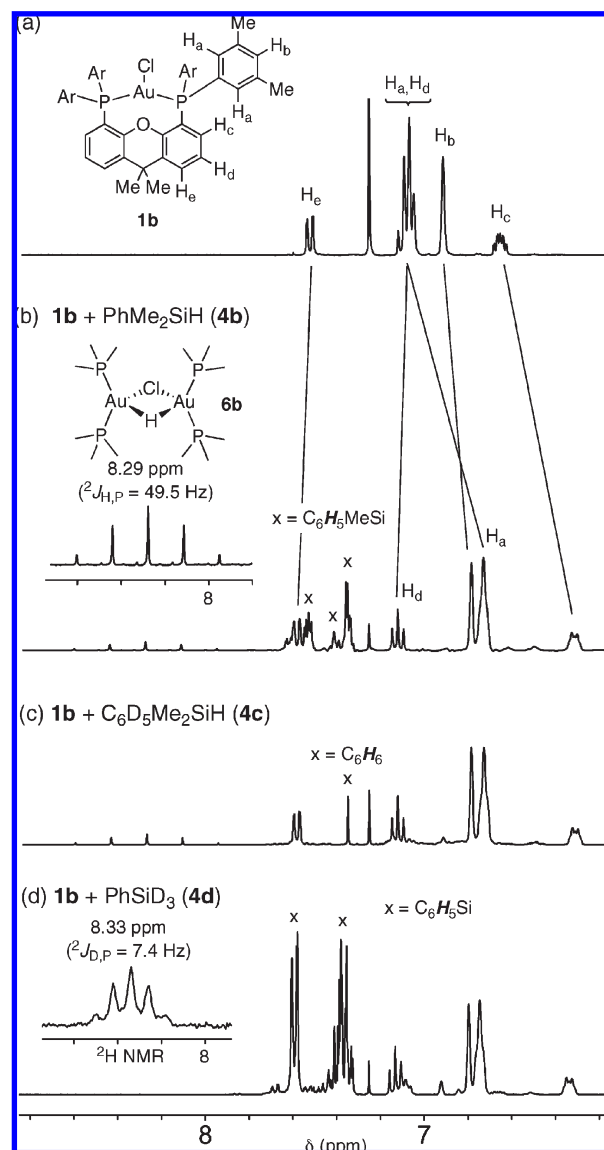


**Figure 5.**  $^1\text{H}$  and  $^2\text{H}$  NMR spectra for gold(I) complexes in  $\text{CDCl}_3$ . (a)  $\text{AuCl}(\text{xy-xantphos})$  (**1b**); (b) **6b** prepared by the reaction between **1b** and  $\text{PhMe}_2\text{SiH}$  (**4b**) (2.0 equiv); (c) **6b** prepared by reaction between **1b** and  $\text{C}_6\text{D}_5\text{Me}_2\text{SiH}$  (**4c**) (2.0 equiv); (d) **6b'** prepared by reaction between **1b** and  $\text{PhSiD}_3$  (**4d**) (5.0 equiv).  $^2\text{H}$  NMR resonance for **6b'** is shown in the inset in (d).

The gold(I) deuteride complex **6b'** was prepared by reacting **1b** with  $\text{PhSiD}_3$  (**4d**) (5 equiv) in a similar manner. In the  $^1\text{H}$  NMR spectrum of the reaction mixture, a set of resonances for the ligand protons was identical with those for **6b**, and the hydride resonance at 8.29 ppm that was observed for **6b** was not observed (Figure 5d). The  $^{31}\text{P}\{^1\text{H}\}$  NMR spectrum of the reaction mixture contains a triplet at 33.5 ppm ( $^2J_{\text{P,D}} = 7.4$  Hz) for **6b'** and a trace signal at 28.7 ppm for unreacted **1b** (Figure 6c). The  $^2\text{H}$  NMR spectrum of **6b'** exhibits the signal for the deuteride ligand as a quintet at 8.33 ppm ( $^2J_{\text{P,D}} = 7.4$  Hz).<sup>30</sup> The ratio between coupling constants of **6b** and **6b'** represents a reasonable value ( $^2J_{\text{P,H}}/^2J_{\text{P,D}} = 6.7$ ) in terms of the gyromagnetic ratio ( $g_{\text{H}}/g_{\text{D}} = 6.5$ ).

Positive ESI mass spectrometry of an acetone/methanol solution of **6b** showed an isomerically resolved peak at

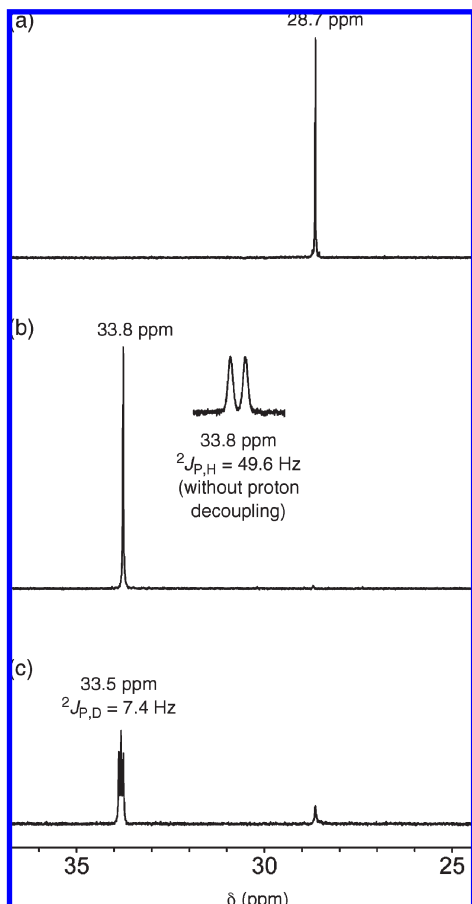


**Figure 6.**  $^{31}\text{P}$  NMR spectra for gold(I) complexes in  $\text{CDCl}_3$ . (a)  $\text{AuCl}(\text{xy-xantphos})$  (**1b**); (b) **6b** prepared by reaction between **1b** and  $\text{PhMe}_2\text{SiH}$  (**4b**) (2.0 equiv);  $^{31}\text{P}$  NMR resonance without proton decoupling; (c) **6b'** prepared by reaction between **1b** and  $\text{PhSiD}_3$  (**4d**) (5.0 equiv).

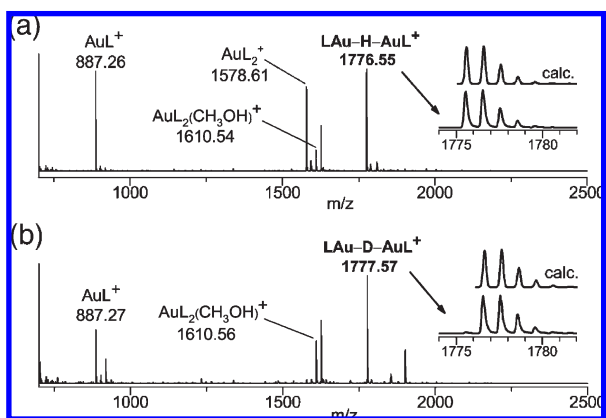


**Figure 7.** ESI-MS for **6b** (a) and **6b'** (b). L = xy-Xantphos.

1776.55, which corresponds to  $[(\text{xy-xantphos})\text{Au}(\mu\text{-H})\text{Au}(\text{xy-xantphos})]^+$  (Figure 7a). A solution of **6b'** showed peaks at 1777.57 for  $[(\text{xy-xantphos})\text{Au}(\mu\text{-D})\text{Au}(\text{xy-xantphos})]^+$  (Figure 7b). In IR measurements of the solution of **6b**, the characterization of the absorbances related to  $\text{Au-H-Au}$  structures failed. Further, in comparing **6b** and **6b'**, a clear assignment of the absorptions bands proved difficult.

The most probable structure for **6b** is an xy-Xantphos-chelating digold structure with hydride- and chloride-brid-

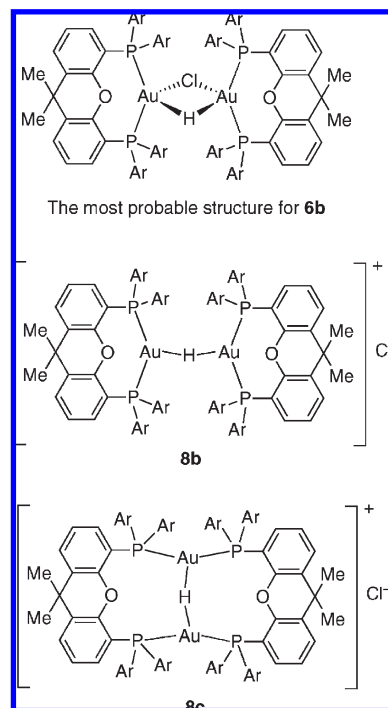


**Figure 8.** Three possible structures for gold(I) hydride species **6b**. Ar = 3,5-dimethylphenyl.

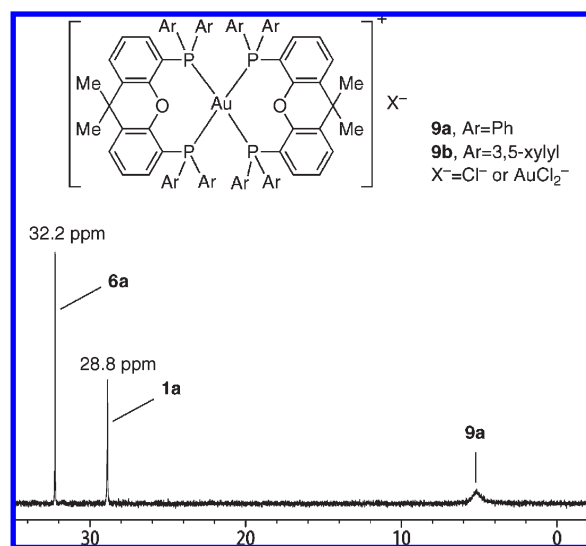


**Figure 9.**  $^{31}\text{P}\{^1\text{H}\}$  NMR spectrum of the reaction mixture of **1a** and **4b** in  $\text{CDCl}_3$ .

ging ligands for the two gold atoms, as illustrated in Figure 8. This structure is consistent with all spectroscopic results described above, although cationic structures, **8b** and **8c**, cannot be excluded as the structure of the gold(I) hydride species.<sup>14e</sup>

The steric bulk of the 3,5-xylyl groups is important for clean formation of the gold(I) hydride complex. Reaction of **1a**, with less bulky phenyl groups on the ligand phosphorus atoms, resulted in the formation of less of the hydride complex, accompanying tetracoordinated cationic complex **9a**, as indicated by the  $^{31}\text{P}\{^1\text{H}\}$  NMR spectrum of the reaction mixture of **1a** and **4b** in  $\text{CDCl}_3$  (Figure 9). A similar side product, **9b**, was not observed in the reaction mixture of **1b** and **4b**. Sterically demanding 3,5-xylyl groups in the



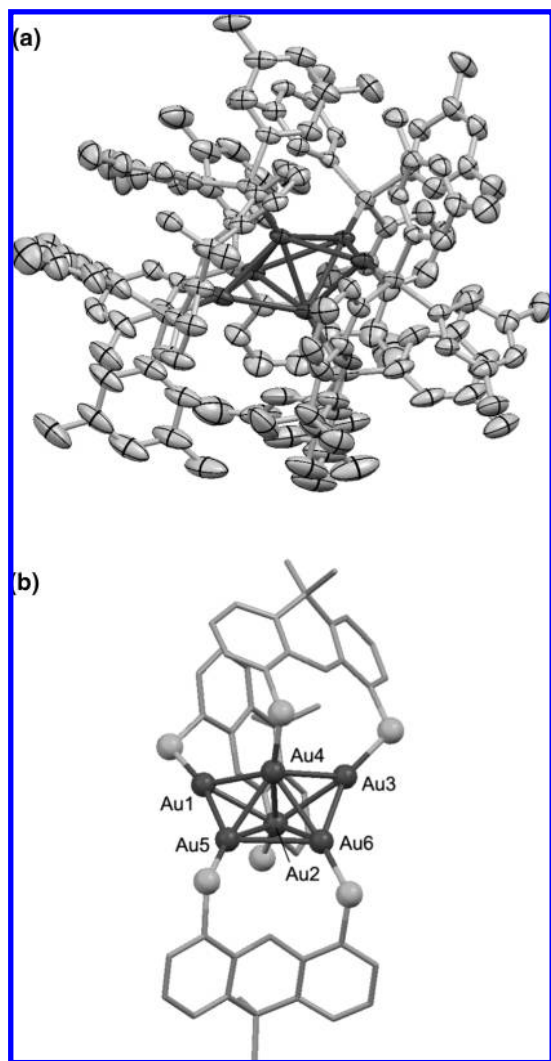
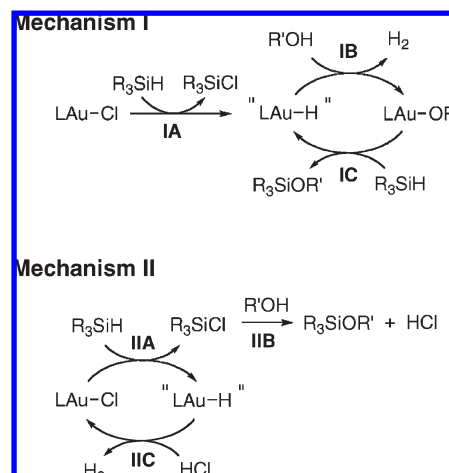


**Figure 10.** (a) ORTEP diagram of  $[\text{Au}_6(\text{xy-xantphos})_3]\text{Cl}$  (**10**) with 50% ellipsoids. Hydrogen and chloride atoms and an inclusion molecule (4-hydroxy-4-methylpentan-2-one) are omitted for clarity. (b) Distorted edge-shared bitetrahedral framework of the  $\text{Au}_6$  core with xanthenes backbone of xy-Xantphos ligands. Gold atoms are depicted as dark gray spheres.

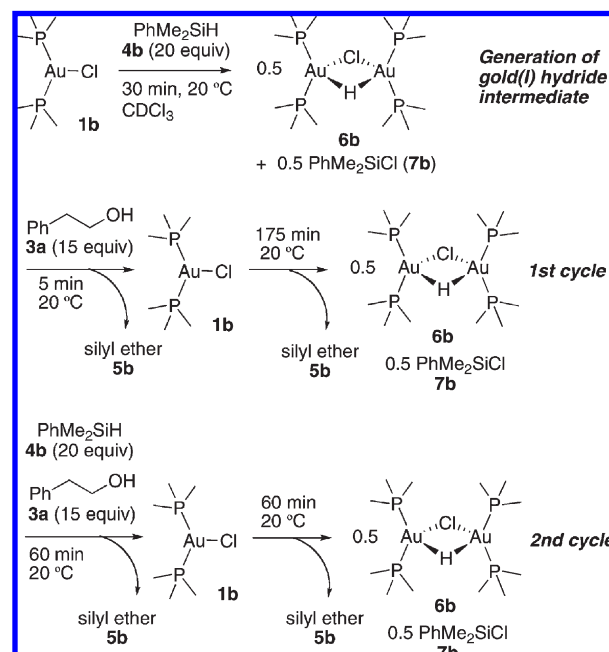
xy-Xantphos ligand are therefore thought to destabilize the congested cationic complex **9b**.

**Formation of  $[\text{Au}_6(\text{xy-xantphos})_3]\text{Cl}$  (**10**).** Isolation of **6b** has not been successfully achieved at present. Addition of hexane to the reaction mixture of **1b** and hydrosilane **4b** resulted in precipitation of **6b** as a pale yellow powder, which consisted of **6b** with a small amount of **1b** and unknown side products. Recrystallization of the yellow powder from acetone/hexane afforded colorless crystals of **1b** and deep red crystals of  $[\text{Au}_6(\text{xy-xantphos})_3]\text{Cl}$  (**10**). The  $^1\text{H}$  and  $^{31}\text{P}$  NMR spectra of these compounds were quite different from those of **6b**. More than 400 crystallization conditions in terms of solvents and temperature were screened, although only **1b** and **10** were obtained as the crystals. X-ray crystallography

**Scheme 4.** Possible Model Mechanisms I and II for Gold(I)-Catalyzed Dehydrogenative Silylation



**Scheme 5.** NMR Monitoring Experiments of Gold(I)-Catalyzed Dehydrogenative Silylation



of **10** revealed the distorted edge-shared bitetrahedral structure of the  $\text{Au}_6$  core with three bridging xy-Xantphos ligands (Figure 10).<sup>31</sup> No hydrogen ligands were present, and five out of six gold(I) atoms were reduced to gold(0), as indicated in the NMR and X-ray crystallography (see Supporting Information). This compound is a dead-end product and has no catalytic activity for the dehydrogenative silylation of alcohols.

**NMR and GC Monitoring of Gold(I) Catalysis.** We considered two different models for reaction mechanisms, in which the gold(I) hydride species is a key intermediate (Scheme 4). In mechanism I, a gold(I) chloride complex ( $\text{LAu-Cl}$ ) first reacts with a hydrosilane to produce a gold(I) hydride (" $\text{LAu-H}$ ") species (**IA**). This gold(I) hydride is converted to a gold(I) alkoxide intermediate via reaction with an alcohol, accompanying evolution of hydrogen (**IB**). The reaction between the gold(I) alkoxide ( $\text{LAu-OR'}$ ) and

(31) For examples of distorted edge-shared tetrahedral  $\text{Au}_6$  clusters, see: (a) van der Velden, J. W. A.; Bour, J. J.; Otterloo, B. F.; Bosman, W. P.; Noordik, J. H. *J. Chem. Soc., Chem. Commun.* **1981**, 583–584. (b) Briant, C. E.; Hall, K. P.; Mingos, D. M. P. *J. Organomet. Chem.* **1983**, 254, C18–C20.

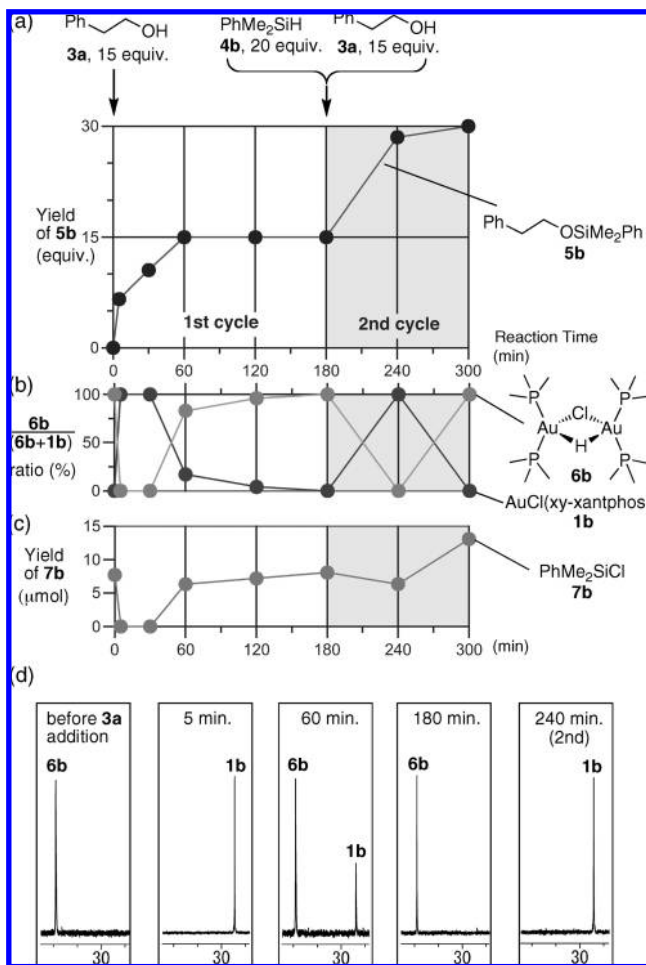


**Figure 11.** NMR monitoring of gold(I)-catalyzed dehydrogenative silylation. Reaction conditions: the first cycle (0–180 min), **1b** (1.0 equiv, 0.0217 mmol), **4b** (20 equiv, 0.434 mmol), and **3a** (15 equiv, 0.325 mmol) at 20 °C under nitrogen in  $\text{CDCl}_3$  (0.6 mL); the second cycle was started by adding **4b** (20 equiv, 0.434 mmol) and **3a** (15 equiv, 0.325 mmol) to the reaction mixture of the first cycle. (a) Yield of the silyl ether **5b**, (b) **6b**/**1b** + **6b** ratio, (c) yield of chlorosilane (**7b**), and (d)  $^{31}\text{P}$  NMR spectra of the reaction mixtures at various reaction times (before **3a** addition, 5, 60, 180, and 240 min).

the hydrosilane proceeds as the last step, resulting in the formation of the silyl ether and regeneration of the gold(I) hydride species (**IC**). In this mechanism, Si–O bond formation occurs in the reaction between the hydrosilane and the gold(I) alkoxide ( $\text{LAu-OR}'$ ). This type of mechanism has been proposed previously.<sup>6a</sup> On the other hand, in mechanism **II**, the gold(I) hydride species, which is produced in the same manner proposed in mechanism **I** (**IIA**), does not react with the alcohol directly. The Si–O bond formation proceeds through the reaction between the chlorosilane and the alcohol (**IIIB**). HCl, which is produced in this alcohol silylation step, then chlorinates the gold(I) hydride species to regenerate the gold(I) chloride complex (**IIIC**).

NMR monitoring experiments were conducted in order to obtain information on the reaction mechanism. Gold(I) hydride intermediate **6b** was first prepared in  $\text{CDCl}_3$  by reaction of **1b** with excess hydrosilane **4b** (20 equiv) (Scheme 5). After complete conversion of **1b** to **6b**, 15 equiv of 2-phenylethanol (**3a**) were added to this **6b**/hydrosilane/

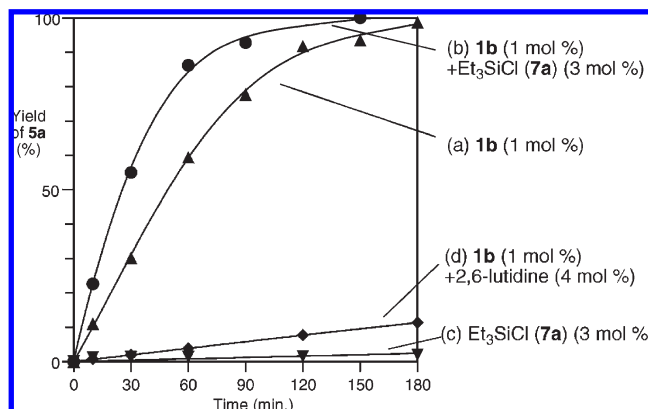
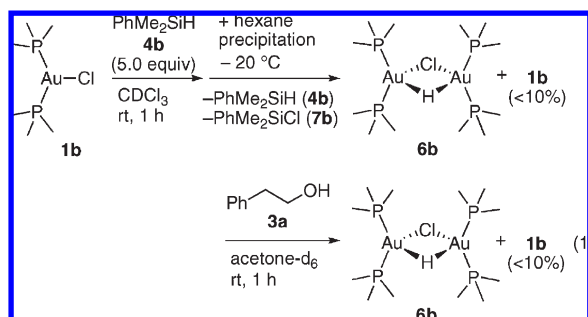


**Figure 12.** Dehydrogenative silylation of 2-phenylethanol (**3a**) with triethylsilane (**4a**) using a catalyst: (a)  $\text{AuCl}(\text{xy-xantphos})$  (**1b**) (1 mol %), (b)  $\text{AuCl}(\text{xy-xantphos})$  (**1b**) (1 mol %),  $\text{Et}_3\text{SiCl}$  (**7a**) (3 mol %), (c)  $\text{Et}_3\text{SiCl}$  (**7a**) (3 mol %), (d)  $\text{AuCl}(\text{xy-xantphos})$  (**1b**) (1 mol %), 2,6-lutidine (4 mol %). Conditions: 1,2-dichloroethane (0.5 mL), 2-phenylethanol (**3a**) (0.5 mmol), catalyst,  $\text{Et}_3\text{SiH}$  (**4a**) (1.0 mmol) at 30 °C. Yield of **5a** was determined by GC using 1,4-diisopropylbenzene as an internal standard.

chlorosilane mixture. **6b** and chlorosilane **7b** quickly disappeared within 5 min, accompanied by production of silyl ether **5b** and regeneration of **1b**, as measured by  $^1\text{H}$  and  $^{31}\text{P}\{^1\text{H}\}$  NMR (Figure 11). Only **1b** was observed as the gold(I) complex in the reaction mixture until alcohol **3a** was consumed (Figure 11b and c; reaction times: 5 and 30 min). **3a** disappeared within 60 min, and the corresponding silyl ether **5b** formed in quantitative yield. After silylation was complete, **1b** gradually reverted to gold(I) hydride **6b**, accompanied by formation of chlorosilane **7b** (Figure 11c; reaction time: 60–180 min). The second catalytic reaction started by addition of alcohol **3a** (15 equiv) and hydrosilane **4b** (20 equiv) to the reaction mixture of the first cycle. In the second cycle, even after an additional 60 min (reaction time: 240 min), the reaction was not complete and only **1b** was observed. Gold(I) hydride complex **6b** was regenerated again after complete consumption of alcohol **3a** (reaction time: 300 min).<sup>32</sup> The gold(I) alkoxide intermediate, which was expected to form in mechanism **I**,<sup>6a</sup> was not detected in any stage of the catalysis. The NMR monitoring experiments indicate that the chlorosilane may participate in the catalytic cycle and play a vital role along with the gold(I) complex, suggesting that mechanism **II** in Scheme 4 is more probable than mechanism **I**.

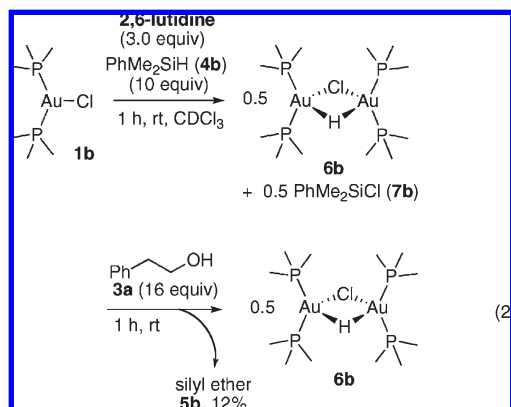
To eliminate the reaction of the chlorosilane, a solution of gold(I) hydride **6b** that did not contain chlorosilane **7b** was prepared. Precipitation by addition of hexane to the reaction mixture of **1b** and **4b** at  $-20$  °C afforded a pale yellow powder of **6b** with very little **1b** (<10%) (eq 1). In the acetone- $d_6$  solution of this product, alcohol **3a** (3.0 equiv) was added at room temperature under argon; gold(I) hydride **6b** remained intact even after 1 h. These results support mechanism **II** in Scheme 4 rather than mechanism **I**, which involves the direct reaction between the gold(I) hydride intermediate and the alcohol.

(32) Under room light, unreacted **4b** was slowly converted to **7b** in the presence of gold hydride **6b** in  $\text{CDCl}_3$ . Although the experiments for Figure 11c were carried out under almost dark conditions, the yields of **7b** at long reaction times (240 and 300 min) probably include the product of this photoinduced side reaction.



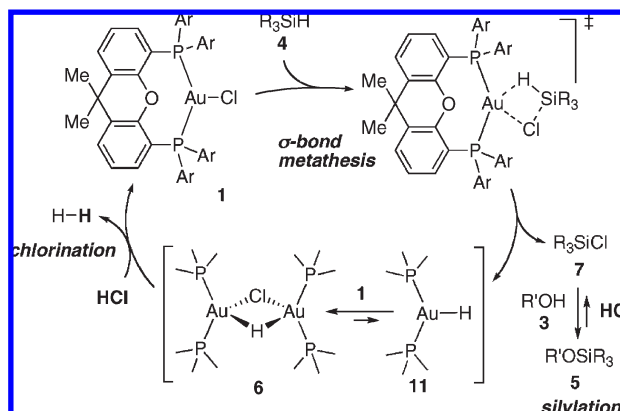
We next examined the effect of adding a chlorosilane and a base on the catalytic activities. Dehydrogenative silylation of 2-phenylethanol (**3a**) (0.5 mmol) with  $\text{Et}_3\text{SiH}$  (**4a**) (1.0 mmol) in 1,2-dichloroethane (0.5 mL) at 30 °C was carried out (Figure 12). Reaction with 1.0 mol % of  $\text{AuCl}(\text{xy-xantphos})$  was almost completed at 180 min (Figure 12a). Addition of a catalytic amount of  $\text{Et}_3\text{SiCl}$  (**7a**) (3 mol %) in the  $\text{AuCl}(\text{xy-xantphos})$  (**1b**) (1.0 mol %) catalytic system resulted in significant acceleration of the reaction rate (Figure 12b), although the use of a catalytic amount of  $\text{Et}_3\text{SiCl}$  (**7a**) (3.0 mol %) resulted in a low yield of the product (2% yield, 3 h) (Figure 12c). It is obvious that the chlorosilane is an important factor for the gold(I)-catalyzed reaction. The effect of a base was examined by adding a catalytic amount of 2,6-lutidine (4.0 mol %) to gold(I) catalyst (**1b**) (1.0 mol %), resulting in a drastic reduction in the reaction rate (11% yield, 3 h) (Figure 12d). Since 2,6-lutidine is a good base but a poor ligand to the gold(I) center, this inhibition may be caused by trapping of HCl generated in the catalytic cycle. These results support mechanism **II**, which involves silylation of the alcohol with chlorosilane and chlorination of gold(I) hydride by HCl.

The results of further NMR monitoring experiments also reveal that 2,6-lutidine inhibits reaction between **6b** and HCl rather than the formation of **6b** and silylation of the alcohol (eq 2). Reaction between gold(I) complex **1b** and 10 equiv of hydrosilane **4b** was carried out in the presence of 3.0 equiv of 2,6-lutidine. The reaction was complete within 1 h to give gold(I) hydride **6b**, similar to the reaction without 2,6-lutidine. This observation suggests that 2,6-lutidine does not affect the gold(I) hydride formation step. Addition of 16 equiv of alcohol **3a** then afforded the corresponding silyl ether in a low yield (12%, based on **3a**), but the gold(I) hydride intermediate remained intact even after 1 h. This is quite different from the reaction without 2,6-lutidine, suggesting that 2,6-lutidine inhibited chlorination of **6b** by trapping HCl.



**Proposed Reaction Mechanism.** Here, we propose a reaction mechanism for the gold(I)-catalyzed dehydro-

**Scheme 6. Proposed Mechanism for Gold(I)-Catalyzed Dehydrogenative Silylation**



genative silylation on the basis of the experimental results described above (Scheme 6). The catalytic cycle starts from the reaction between **1** and **4** through  $\sigma$ -bond metathesis. Monomeric gold(I) hydride **11** that should be produced by the metathesis reaction is trapped by **1**, forming dinuclear gold(I) hydride complex **6**. Chlorosilane **7**, which is the counterpart of the gold(I) hydride in the first metathesis reaction, reacts with alcohol **3** to form silyl ether **5**, accompanied by release of HCl. The gold(I) hydride complexes (**6** or **11**) are then chlorinated by HCl to regenerate **1** with evolution of hydrogen gas. The silylation step would include the equilibrium with desilylation, but the rapid reaction of HCl with **6b** shifts the equilibrium to silyl ether production. The  $\sigma$ -bond metathesis is expected to be the slowest step in the catalytic cycle. This explains the fact that only **1b** was observed during the catalytic reaction in the NMR monitoring experiment. After the alcohol was consumed, gold(I) hydride **6b** was observed because HCl was no longer produced and the chlorination step does not occur.

## Summary

Dimeric gold(I) hydride complexes were generated by reaction of gold(I) chloride complexes (**1a** and **1b**) and hydrosilanes. The reaction mechanism for the gold(I)-catalyzed dehydrogenative silylation of alcohols involving a gold(I) hydride intermediate was proposed, based on NMR experiments and mechanistic studies. The outstanding activities of  $\text{AuCl}(\text{xantphos})$  (**1a**) and  $\text{AuCl}(\text{xy-xantphos})$  (**1b**) compared with those of other  $\text{AuCl}/\text{phosphine}$  combinations can be explained by the high stability of the tricoordinated structure around the gold atom in the Xantphos and xy-Xantphos complex. The activation of the Au–Cl bond induced by the stereoelectronic effect of the two chelating phosphorus atoms of Xantphos and the xy-Xantphos ligands is crucial for  $\sigma$ -bond metathesis in the first step. The steric bulk of xy-Xantphos prevents the formation of a cationic tetracoordinated gold(I) complex. This explains the higher reactivity of  $\text{AuCl}(\text{xy-xantphos})$  (**1b**) than that of  $\text{AuCl}(\text{xantphos})$  (**1a**).

The gold(I) hydride intermediate is relatively inert and does not react directly with alcohols. This low reactivity is important for functional group compatibility of the gold(I)-catalyzed dehydrogenative silylation. Si–O bond formation in the catalysis relies on the reaction between



the alcohol and the chlorosilane formed by the reaction between the gold(I) chloride complexes and the hydrosilanes. HCl is generated along with the silylation step and is used in the subsequent chlorination of the gold(I) hydride to regenerate the gold(I) chloride complexes. Further structural studies by X-ray crystallography as well as more detailed kinetic experiments are necessary; however, our present analysis clearly demonstrates that the gold(I) hydride intermediate also plays an essential role in catalysis. This study is expected to generate interest in gold(I) hydrides as catalysts.

## Experimental Section

**General Considerations.** Materials were obtained from commercial suppliers and purified by the standard procedure unless otherwise noted. Solvents were purchased from commercial suppliers, degassed via three freeze–pump–thaw cycles, and further dried on MS4A. Xantphos and DBFphos were prepared according to the literature.<sup>19</sup> Other phosphine ligands were purchased from commercial suppliers and used without further purification. AuCl(xy-xantphos) (**1a**) was prepared according to the procedure described before.<sup>6a</sup> PhSiD<sub>3</sub> (**4d**) was prepared from PhSiCl<sub>3</sub> by reduction with LiAlD<sub>4</sub>.<sup>33</sup> 1,4-Diisopropylbenzene was distilled from CaH<sub>2</sub> and stored on MS4A under an atmosphere of argon.

NMR spectra were recorded on a Varian Gemini 2000 (<sup>1</sup>H: 300 MHz, <sup>31</sup>P: 121.4 MHz, and <sup>13</sup>C: 75.4 MHz) spectrometer and a JEOL JNM-ECA600 (<sup>1</sup>H: 600 MHz, <sup>31</sup>P: 242.8 MHz) spectrometer. Tetramethylsilane (<sup>1</sup>H) and CDCl<sub>3</sub> (<sup>31</sup>C) were employed as external standards, respectively. Phosphoric acid (85%) was employed as an external standard for <sup>31</sup>P NMR measurement. Gas chromatographic (GLC) analyses were conducted on a Shimadzu GC-14B equipped with a flame ionization detector. IR spectra were recorded on a Perkin-Elmer Spectrum One. Low- and high-resolution mass spectra were recorded on a JEOL JMS-700TZ mass spectrometer at the Center for Instrumental Analysis, Hokkaido University.

**X-ray Crystallography.** The data for **1a** and **1b** were collected on a Rigaku/MS Mercury CCD diffractometer. The data for **10** were collected using a Rigaku Saturn 724 CCD diffractometer. Cell constants and an orientation matrix for data collection were obtained. All of the data were corrected for Lorentz and polarization effects. A summary of the cell parameters, data collection conditions, and refinement results is given in the Supporting Information. The structures were solved by direct methods<sup>34a</sup> and expanded using Fourier techniques.<sup>34b</sup> All calculations were performed using the teXsan crystallographic software package.<sup>34c</sup> Crystallographic data have been deposited with Cambridge Crystallographic Data Centre: deposition numbers CCDC-740701, CCDC-740702, and CCDC-740700 for **1a**, **1b**, and **10**, respectively. Copies of the data can be obtained free of charge via <http://www.ccdc.cam.ac.uk/conts/retrieving.html> (or from the Cambridge Crystallographic Data Centre, 12 Union Road, Cambridge, CB2 1EZ, UK; fax: +44 1223 336033; e-mail: [deposit@ccdc.cam.ac.uk](mailto:deposit@ccdc.cam.ac.uk)).

**Synthesis of 4,5-Bis[bis(3,5-dimethylphenyl)phosphino]-9,9-dimethylxanthene (xy-Xantphos) (**2b**).** In a round-bottomed three-

necked flask equipped with a stopcock, a rubber septum, and an addition funnel, a solution of 3,5-dimethylphenyllithium was prepared by addition of a solution of *n*-BuLi (36.7 mL of a 1.52 M solution in hexane, 55.8 mmol) to a solution of 1-bromo-3,5-dimethylbenzene (10.3 g, 55.8 mmol) in 40 mL of Et<sub>2</sub>O at –78 °C under argon. In another flask, a THF solution (15 mL) of 4,5-bis(diethoxyphosphino)-9,9-dimethylxanthene was prepared from 9,9-dimethoxyxanthene (2.0 g, 9.52 mmol) and diethyl chlorophosphite (3.0 mL, 3.29 g, 21.0 mL) according to the reported procedure.<sup>18a</sup> This solution was transferred into the addition funnel via a Teflon tube and was slowly added to the solution of 3,5-dimethylphenyllithium at –78 °C. The mixture was then allowed to warm to room temperature and stirred overnight. After the solvent was removed in vacuo, 20 mL of degassed water and 40 mL of degassed dichloromethane were added to the residual oil. After vigorous stirring, the organic layer was separated and dried over MgSO<sub>4</sub> under an argon atmosphere. Evaporation of the solvent gave a yellow solid, which was purified by column chromatography using argon-bubbled solvents (SiO<sub>2</sub>, hexane/diethyl ether, 98:2) to give **2b** as a white solid (3.41 g, 36.7 mmol, 52%). <sup>1</sup>H NMR (300 MHz, CDCl<sub>3</sub>, δ): 1.64 (s, 6H, C(CH<sub>3</sub>)<sub>2</sub>), 2.17 (s, 24H, ArCH<sub>3</sub>), 6.54 (brd, *J*<sub>P,C</sub> = 7.4 Hz, 2H), 6.78 (brs, 8H), 6.84 (s, 4H), 6.96 (t, *J*<sub>P,C</sub> = 7.7 Hz, 2H), 7.38 (d, *J*<sub>P,C</sub> = 7.7 Hz, 2H). <sup>31</sup>P{<sup>1</sup>H} NMR (121.4 MHz, CDCl<sub>3</sub>, δ): –16.8. <sup>13</sup>C{<sup>1</sup>H} NMR (75.4 MHz, CDCl<sub>3</sub>, δ): 21.2 (CH<sub>3</sub>), 30.9 (CH<sub>3</sub>), 34.5 (t, *J*<sub>P,C</sub> = 1.7 Hz, C), 123.3 (CH), 125.6 (CH), 126.40–12.68 (m, C), 129.9 (CH), 130.2 (C), 131.6 (t, *J*<sub>P,C</sub> = 10.6 Hz, CH), 132.0 (C), 137.1 (t, *J*<sub>P,C</sub> = 3.7 Hz, CH), 137.24–137.41 (m, C), 153.1 (t, *J*<sub>P,C</sub> = 9.7 Hz, C). IR (neat, cm<sup>–1</sup>): 2915 (m), 1401 (s), 1228 (s). APCI-MS (*m/z*): [M + H]<sup>+</sup> calcd for C<sub>47</sub>H<sub>48</sub>OP<sub>2</sub>, 691.3259; found, 691.3263.

**Synthesis of AuCl(xy-xantphos) (**1b**).** AuCl(SMe<sub>2</sub>) (235 mg, 0.80 mmol) and xy-Xantphos (**2b**) (551 mg, 0.80 mmol) were placed in a 20 mL round-bottomed flask. The flask was evacuated and backfilled with argon, and dry THF (8.0 mL) was then added with stirring. After 8 h, the solvent was removed in vacuo. The crude product was purified by column chromatography using argon-bubbled solvents (SiO<sub>2</sub>, chloroform/methanol, 97.5:2.5) to give **1b** as a white solid (718 mg, 0.78 mmol, 52%).

<sup>1</sup>H NMR (300 MHz, CDCl<sub>3</sub>, δ): 1.68 (s, 6H, C(CH<sub>3</sub>)<sub>2</sub>), 2.19 (s, 24H, ArCH<sub>3</sub>), 6.64–6.69 (m, 2H, Ar), 6.93 (brs, 4H), 7.06–7.13 (m, 10H), 7.53 (dd, *J* = 1.4, 6.3 Hz, 2H). <sup>31</sup>P{<sup>1</sup>H} NMR (121.4 MHz, CDCl<sub>3</sub>, δ): 28.6. <sup>13</sup>C{<sup>1</sup>H} NMR (75.4 MHz, CDCl<sub>3</sub>, δ): 21.1 (CH<sub>3</sub>), 27.4 (CH<sub>3</sub>), 35.6 (t, *J*<sub>P,C</sub> = 1.6 Hz, C), 119.8 (t, *J*<sub>P,C</sub> = 18.9 Hz, C), 124.5 (t, *J*<sub>P,C</sub> = 3.1 Hz, CH), 126.4 (CH), 131.5 (t, *J*<sub>P,C</sub> = 8.6 Hz, CH), 131.7 (C), 131.9 (CH), 132.8 (t, *J*<sub>P,C</sub> = 22.9 Hz, C), 134.0 (t, *J*<sub>P,C</sub> = 1.7 Hz, C), 137.9 (t, *J*<sub>P,C</sub> = 5.7 Hz, CH), 155.2 (t, *J*<sub>P,C</sub> = 5.2 Hz, C). IR (neat, cm<sup>–1</sup>): 2919 (m), 1401 (s), 1224 (s). APCI-MS (*m/z*): [M + Cl]<sup>+</sup> calcd for C<sub>47</sub>H<sub>48</sub>AuOP<sub>2</sub>, 887.2846; found, 887.2871. Anal. Calcd for C<sub>47</sub>H<sub>48</sub>AuClOP<sub>2</sub>: C, 61.14; H, 5.24. Found: C, 60.84; H, 5.38.

**General Procedure for Gold(I)-Catalyzed Dehydrogenative Silylation (Table 2, Figure 12).** AuCl(xy-xantphos) (4.6 mg, 0.005 mmol) was placed in a reaction vial connected with a argon line through a needle. The vial was vacuumed and back-filled with argon, and a solvent (0.5 mL) was added with stirring. An alcohol (0.5 mmol), a hydrosilane (1.0 mmol), and an internal standard (1,4-diisopropylbenzene, typically 20 mg) were added to the vial at the reaction temperature. A small portion (20 μL) of the reaction mixture was taken from the reaction mixture with a syringe and was passed through a short column of alumina with diethyl ether as an eluent to give a sample for GC analysis. The yields of the product during the reaction were determined by GC analysis of this sample. After the reaction was complete, the reaction mixture was directly subjected to column chromatography (SiO<sub>2</sub>, hexane/ethyl acetate, 100:0–95:5) to give the corresponding silyl ether.

(33) Miura, K.; Tomita, M.; Yamada, Y.; Hosomi, A. *J. Org. Chem.* **2007**, *72*, 787–792.

(34) For X-ray crystallography: (a) Altomare, A.; Cascarano, G.; Giacovazzo, C.; Guagliardi, A.; Burla, M. C.; Polidori, G.; Camalli, M. *J. Appl. Crystallogr.* **1994**, *27*, 435. (b) DIRDIF94: Beurskens, P. T.; Admirals, G.; Beurskens, G.; Bosman, W. P.; de Gelder, R.; Israel, R.; Smits, J. M. M. *The DIRDIF-94 Program System, Technical Report of the Crystallography Laboratory*; University of Nijmegen, **1994**. (c) *teXsan, Crystal Structure Analysis Package*; Molecular Structure Corporation, **1985** and **1999**.



**Synthesis of  $C_6D_5Me_2SiH$  (**4c**).** A THF solution of 2,3,4,5,6-pentadeuteriophenylmagnesium bromide was prepared from magnesium turnings (0.528 g, 21.7 mmol) and 1-bromo-2,3,4,5,6-pentadeuteriobenzene (2.09 mL, 3.23 g, 20 mmol) in dry THF (40 mL) under an atmosphere of argon. Chlorodimethylsilane (2.8 mL, 3.21 g, 34 mmol) was added to the stirred solution via a syringe. After 24 h, the reaction mixture was quenched by addition of 20 mL of water, extracted three times with hexane. The combined organic layer was washed with aqueous NaCl and  $NaHCO_3$  and dried over  $K_2CO_3$ . The distillation of the solution gave **4c** as a colorless oil (1.83 g, 12.95 mmol, 62%).  $^1H$  NMR (300 MHz,  $CDCl_3$ ,  $\delta$ ): 0.37 (d,  $J = 3.6$  Hz, 6H), 4.45 (septet,  $J = 3.8$  Hz, 1H).  $^{13}C$  NMR (75.4 MHz,  $CDCl_3$ ,  $\delta$ ): -3.8, 127.6 (t,  $^1J_{C,D} = 24.6$  Hz), 129.0 (t,  $^1J_{C,D} = 24$  Hz), 133.9 (t,  $^1J_{C,D} = 23.5$  Hz), 137.5. HRMS-ESI ( $m/z$ ):  $[M +]^+$  calcd for  $C_8H_7D_5Si$ , 141.1022; found, 141.1025.

**Synthesis of Gold(I) Hydride Complex **6b**.** Dry, degassed  $CDCl_3$  was passed through an  $Al_2O_3$  short column before use. In a glovebox, a solution of  $AuCl(xy-xantphos)$  (**1b**) (25 mg, 0.027 mmol) in  $CDCl_3$  (0.6 mL) was prepared in a screw-cap NMR sample tube and sealed with an open top cap and Teflon-coated rubber septum. The sample tube was then removed from the glovebox, and  $PhMe_2SiH$  (**4b**) (7.4 mg, 0.054 mmol) or  $C_6D_5Me_2SiH$  (**4c**) (7.6 mg, 0.054 mmol) was then added to the solution in the dark. The sample was shaken and kept at 20 °C. After 30 min, the solution turned red and was subjected to NMR measurements.  $^1H$  NMR (300 MHz,  $CDCl_3$ ,  $\delta$ ): 1.71 (s, 12H,  $C(CH_3)_2$ ), 1.85 (s, 48H,  $ArCH_3$ ), 6.32–6.34 (m, 4H, Ar), 6.74 (brs, 16H), 6.80 (brs, 8H), 7.11–7.16 (t,  $J = 6.3$ , 1.4 Hz, 4H), 7.58–7.61 (d,  $J = 7.7$  Hz, 4H), 7.96–8.62 (quintet,  $^2J_{H,P} = 48.9$  Hz, 1H, Au–H–Au).  $^{31}P\{^1H\}$  NMR (121.4 MHz,  $CDCl_3$ ,  $\delta$ ): 33.8.  $^{31}P$  NMR (121.4 MHz,  $CDCl_3$ ,  $\delta$ ): 33.8 (d,  $^2J_{P,H} = 48.9$  Hz). HRMS (ESI) ( $m/z$ ):  $[M - Cl]^+$  calcd for  $C_{94}H_{97}Au_2O_2P_4$ , 1775.58; found, 1775.55. Precipitation from the reaction mixture prepared from **1b** and **4b** was carried out by adding dry,

degassed hexane in the dark at -20 °C to give a yellow powder of **6b** with a small amount of **1b** (<10%). Gold(I) deuterium complex **6b'** was prepared according to a similar procedure by using  $PhSiD_3$  (**4d**) (15 mg, 0.135 mmol).

**Synthesis of  $[Au_6(xy-xantphos)_3]Cl$  (**10**).** In a glovebox, the yellow powder of **6b** (100 mg, 0.0552 mmol) that was prepared according to the above procedure was dissolved in dry acetone (1.0 mL). Dibutyl ether or hexane (5.0 mL) was added slowly onto the solution. Crystallization was carried out at 4 °C in the dark to give  $[Au_6(xy-xantphos)_3]Cl$  (**10**) in 35% yield as red prisms. The crystals included 4-hydroxy-4-methylpentan-2-one. See Supporting Information for the  $^1H$  and  $^{31}P$  NMR spectra. A product that was prepared from **1b** and deuteriosilane **4d** was identical to **10** as judged by  $^1H$  and  $^2H$  NMR. HRMS (ESI) ( $m/z$ ):  $[M - Cl]^+$  calcd for  $C_{141}H_{144}Au_6O_3P_6$ , 1626.38; found, 1626.34. Anal. Calcd for  $C_{147}H_{156}Au_6ClO_5P_6$ : C, 51.84; H, 4.62. Found: C, 51.55; H, 5.14.

**Acknowledgment.** This work was supported by a Grant-in-Aid for Scientific Research (B) (No. 20350043) from Japan Society for the Promotion of Science (JSPS). This work was also supported by PRESTO of the Japan Science and Technology Agency (JST). The authors thank Prof. Tamotsu Inabe and Prof. Takanori Suzuki for the X-ray crystallographic analysis of **1a**, **1b**, and **10**. Rigaku Corporation is also acknowledged for the single-crystal X-ray analysis of **10**. The authors also thank Prof. Seiji Mori for helpful discussions.

**Supporting Information Available:** Details of X-ray crystallographic analysis of **1a**, **1b**, and **10**. Full-scale  $^1H$ ,  $^{13}C$ , and  $^{31}P$  NMR spectra of **1a**, **1b**, **6b**, and **6b'**. HETCOR(H/P) spectrum of **6b**.  $^2H$  NMR spectrum of **6b'**. These materials are available free of charge via the Internet at <http://pubs.acs.org>.